

Influence of Deposition and Annealing Parameters on the Degradation of Spray-Deposited Perovskite Films

Gabriel Bartholazzi^a , Robson Pacheco Pereira^a , Leila Rosa Cruz^{a*} 

^aInstituto Militar de Engenharia, Praça General Tibúrcio, Urca, 22290-270, Rio de Janeiro, RJ, Brasil.

Received: January 13, 2021; Revised: July 7, 2021; Accepted: July 13, 2021

In this work, $\text{CH}_3\text{NH}_3\text{PbI}_3$ perovskite thin films were deposited by the spray-coating method in ambient conditions using different deposition temperatures and annealing times. They were then exposed to high humidity in order to investigate the relation between processing parameters and degradation mechanisms. FTIR and XRD analyses identified two degradation mechanisms, one reversible, the formation of monohydrated perovskite, $\text{CH}_3\text{NH}_3\text{PbI}_3 \cdot \text{H}_2\text{O}$, and another irreversible, the decomposition of perovskite into PbI_2 and $\text{CH}_3\text{NH}_3\text{I}$. It was found that perovskite degradation is very sensitive to deposition parameters and that long annealing times at high temperatures increase compound stability, retarding reversible degradation even after a long exposure to ambient conditions. This is attributed to the formation of a small amount of PbI_2 during deposition that acts as a protective layer against moisture, preventing the formation of monohydrated perovskite. Additionally, no signs of dihydrated perovskite were found in the films even after 50 days of exposure to high humidity.

Keywords: Perovskite films, reversible and irreversible degradation, spray deposition.

1. Introduction

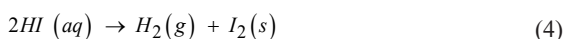
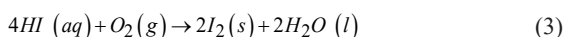
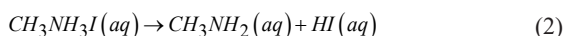
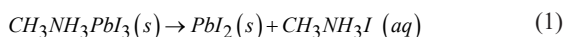
The efficiency of perovskite solar cells has increased considerably over the past few years, reaching the value of 25.5%¹. They employ an absorber layer made with a compound with the same crystal structure as the mineral perovskite, CaTiO_3 , which can be described by the chemical formula ABX_3 , where A is a cation, B is a metal and X is a halide. Different ABX_3 components can be used, leading to perovskites with different properties². Methylammonium lead iodide ($\text{CH}_3\text{NH}_3\text{PbI}_3$) is one of the most employed perovskites due to excellent optoelectronic properties such as band gap of 1.5 eV, which results in an absorption onset near the edge of the visible light spectrum, large carrier diffusion lengths for both electrons and holes (up to 1 μm when doped with chloride), high absorption coefficient, and low carrier recombination rates³⁻⁶.

This compound can be produced by several techniques, from the complex physical vapour deposition to the simple spin coating^{1,7,8}. Despite being widely employed, the one-step spin coating deposition yields films with poor coverage and needle-like morphology that compromise device efficiency⁹⁻¹¹. In order to overcome this problem, a solvent-engineering step and/or a two-step deposition is required to achieve the desired morphology and coverage¹²⁻¹⁴.

Currently, perovskite solar cells face two main challenges: scalability and stability. Since spin coating is not a scalable technique, it must be replaced by a method that can produce good quality films over large areas. A technique that has received some attention in the literature is spray deposition^{10,11,15-18}. In this method, a precursor solution passes through a nozzle

that breaks the liquid into small droplets, which are deposited onto a substrate. The surface characteristics of the film, such as uniformity and coverage, depend greatly on the contact angle, which must be low enough to assure good wettability^{19,20}. An important advantage of the spray coating method is the possibility of heating the substrate during deposition. Heating the substrates improves wettability by reducing the fluid surface tension²⁰. Substrate heating also increases the solvent evaporation rate, decreasing deposition time^{15,17}.

As for stability, perovskite films are susceptible to fast degradation by external agents such as moisture, oxygen, and ultraviolet radiation²¹⁻²³. The degradation is initiated by moisture, which hydrolyzes $\text{CH}_3\text{NH}_3\text{PbI}_3$ (Equations 1 and 2) and proceeds according to Equation 3 or Equation 4, depending on whether HI is decomposed by oxygen or UV radiation²³. The solid end-products of this irreversible process are PbI_2 and I_2 . Most of the existing studies of stability address different ways to prevent this type of degradation²⁴⁻²⁶.



Little attention, however, has been given to a different degradation mechanism that may occur when the perovskite

*e-mail: leilacruz@ime.br

is exposed to humidity²⁷. In this process, a water molecule is added to perovskite to form monohydrated methylammonium lead iodide ($\text{CH}_3\text{NH}_3\text{PbI}_3 \cdot \text{H}_2\text{O}$)²⁷⁻²⁹. The main feature of this degradation mechanism is its reversibility. Perovskites that undergo reversible degradation are converted back to the original structure upon exposure to vacuum, temperature or low-humidity atmosphere^{30,31}. Christians et al.³⁰ reported films with low roughness and highly oriented monohydrated crystal structure where reversible degradation took place. In addition to changes in structure and morphology, reversible degradation changes the typical dark grey appearance of perovskite films to a transparent one as the band gap shifts from the usual value of 1.5 eV to 3.1 eV after exposure to high humidity²⁷.

In the case of long exposure times, this perovskite hydration may be followed by a second one to form dihydrated methylammonium lead iodide, $(\text{CH}_3\text{NH}_3)_4\text{PbI}_6 \cdot 2\text{H}_2\text{O}$ ³². Yang et al.²⁸ regard the formation of monohydrated and dihydrated perovskites as intermediate steps of irreversible degradation, while, according to Leguy et al.²⁷, reversible and irreversible processes follow independent paths.

Although perovskite degradation has been extensively investigated, the correlation between the manufacturing process and the degradation mechanism is not well understood. In a previous work³³, we determined the best conditions to rapidly deposit and crystallize sprayed $\text{CH}_3\text{NH}_3\text{PbI}_3$ perovskite thin films in a single step. Crystalline films with high coverage and large equiaxed grains (4-5 μm) were obtained in a very short annealing time (30 s) at 120 °C. In this work, the focus is on the degradation mechanisms. Perovskite films were prepared in ambient conditions, under different deposition temperatures and annealing times, and were exposed to high humidity for long times in order to investigate the relation between processing parameters and degradation mechanisms.

2. Material and Methods

A commercial spray gun, Steula BC 66-08 airbrush, with 0.8-mm nozzle size, was incorporated in a homemade automatic system to provide better reproducibility³³. The system was based on a solenoid and a computer software, which was used to control the deposition time and pull the airbrush trigger. The spray gun was placed 10 cm away from a hotplate in a perpendicular position. A graphite block was placed on the hotplate to homogenize the temperature throughout deposition. Fluorine-doped tin oxide (FTO) glass substrates were cleaned by ultrasonication in a diluted detergent solution at 60 °C and rinsed in distilled water and isopropanol before drying in a chamber with an IR lamp. The 1 cm^2 substrates were placed onto the graphite block at temperatures ranging from 80 °C to 120 °C. The perovskite solution was prepared using lead iodide (PbI_2) and methylammonium iodide ($\text{CH}_3\text{NH}_3\text{I}$) diluted in anhydrous dimethylformamide (DMF). All chemicals were P.A. grade from Sigma Aldrich. The precursors were diluted in DMF to obtain a 10 wt.% solution. The solution was stirred at 60 °C in ultrasonic bath for 30 min before being filtered in a 0.2 μm PTFE filter and placed in the airbrush cup. After the substrates reached the deposition temperature, the solution was sprayed for 1 s, using N_2 carrier gas at 5 psi. Immediately after deposition, the samples were kept at the same temperature on the hotplate for annealing.

Table 1 shows the annealing parameters. Under these conditions, the thickness of the films was roughly 2 μm . Low deposition temperatures and short annealing times were chosen to avoid thermal degradation without compromising film crystallization³³.

To investigate the relation between processing parameters and perovskite degradation, a set of samples - herein called 24-h films - was kept for 24 h in high-humidity ambient conditions (80% in average). The 24-h films that contained the monohydrate phase underwent a 10 s heat treatment at 100 °C to evaluate the conversion back to perovskite. The 24-h films were again exposed to humidity for 50 days (50-day films) and then the monohydrate-containing films were submitted to the conversion heat treatment. Perovskite degradation and reversibility were evaluated by X-ray diffraction (XRD) in a D8 Advanced diffractometer; Cu-K α radiation, 0.02 s^{-1} scan rate and a 0.1° step size were employed. Fourier Transformed Infrared (FTIR) spectroscopy was performed in a Thermo Nicolet iS50 FTIR spectrometer, with a Harrick Praying Mantis diffuse reflectance accessory. The reflectance (R) was collected with a resolution of 4 cm^{-1} (32 scans) ranging from 400 cm^{-1} to 4000 cm^{-1} . Scanning Electron Microscopy (SEM) images were collected in a Quanta scanning electron microscope with field emission gun.

3. Results and Discussion

Figure 1 shows the XRD patterns of perovskite films deposited at different temperatures and times after the first 24 h of exposure to ambient conditions. The diffractograms of these 24-h films exhibit the most intense diffraction peaks of tetragonal perovskite at 14.0°, 19.85°, 23.45°, 24.17°, 28.33°, 31.77°, 40.93°, and 49.64°, corresponding respectively to the (002)/(110), (112)/(200), (211), (202), (004)/(220), (114), (224)/(400), and (404) diffraction planes³⁴. Moreover, it can be seen that a 24 h exposure to high humidity was enough to reversibly degrade the perovskite films deposited at 80 °C, irrespective of the annealing time, as can be confirmed by the presence of the monohydrate perovskite phase, identified by the peaks at 10.46° and 16.03°^{27,30,31}. Samples prepared at higher deposition temperatures and shorter annealing times presented a similar behaviour, that is, the XRD patterns of the 24-h films deposited at 100 °C and 110 °C showed the monohydrate phase peaks only when the annealing time was less than 30 s, while those of the samples deposited at 120 °C presented the monohydrate phase peaks for annealing times below 10 s. The perovskite films that were annealed for the shortest period of time (100 °C for 30 s; 110 °C for 10 s and 120 °C for 5 s) degraded the most with almost no remaining traces of perovskite. XRD patterns of some of these samples, obtained right after deposition, are shown in a previous work³³; no monohydrate phase was observed in the

Table 1. Deposition temperatures and annealing times of the $\text{CH}_3\text{NH}_3\text{PbI}_3$ perovskite films.

Temperature	Annealing time				
	30 s	-	10 min	-	-
80 °C	30 s	1 min	3 min	-	-
100 °C	30 s	1 min	3 min	-	-
110 °C	30 s	1 min	3 min	-	-
120 °C	5 s	10 s	15 s	20 s	30 s

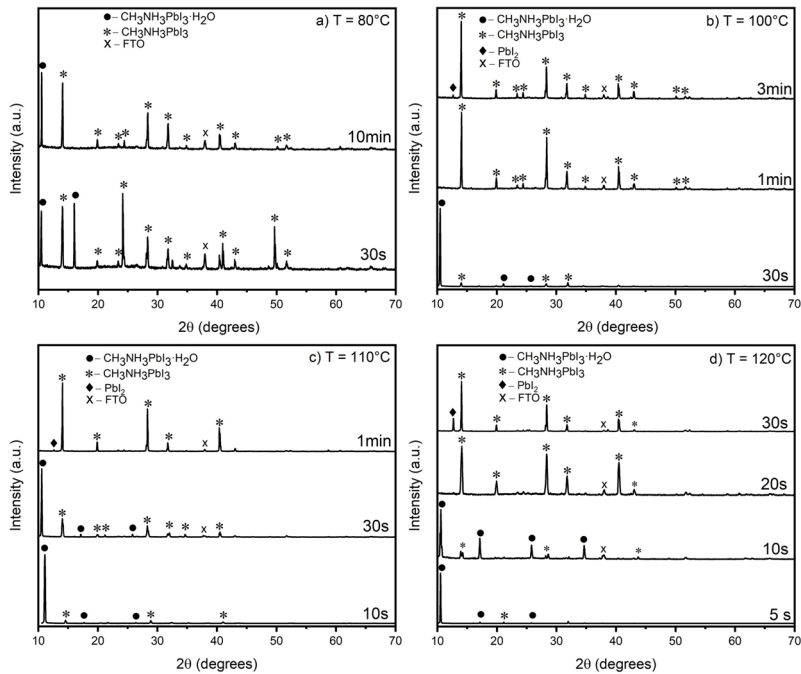


Figure 1. XRD patterns of the perovskite 24h-films fabricated via spray deposition at different temperatures and annealing times: a) 80 °C; b) 100 °C; c) 110 °C; d) 120 °C.

films, confirming that it is due to humidity. On the other hand, films produced at higher temperatures and longer annealing times did not exhibit the monohydrate phase. These results show that high temperatures and long annealing times lead to better stability of perovskite films over the first 24 h, and the reason for this might be associated with the deposition technique employed.

Due to the high temperatures involved, the spray deposition enables the production of highly crystalline perovskite films in a time shorter than other techniques, such as spin coating¹⁷. The high temperature, in turn, can also lead to partial irreversible degradation, with the presence of PbI_2 , as can be seen by the small peak at 12.68° in Figure 1³⁵. Although the presence of PbI_2 in perovskite layers should be avoided, our results suggest that the formation of a small quantity of this inorganic compound may contribute to the stability of the perovskite layer, since the appearance of the PbI_2 phase coincided with the disappearance of the monohydrate phase. When methylammonium elimination takes place at the surface, a PbI_2 layer is formed, protecting the inner layers of the film from moisture-induced degradation. This is in accordance with a previous study that suggests that perovskite layers produced from a solution with excess PbI_2 are more stable³⁶.

It is also worth mentioning a study carried out by Wang et al.²⁹ that correlates moisture-induced degradation and film microstructure. They argued that since moisture infiltrates the film through grain boundaries, a microstructure composed of large grains might improve film stability. Therefore, samples annealed at higher temperatures during long times are more resistant to moisture infiltration because they have larger grains. Indeed, in a previous paper³³ we observed that grain size increased with annealing temperature, but SEM

images of perovskite films deposited at 120 °C (Figure 2) indicates that grain size was not affected by annealing time.

Figure 3 shows the XRD patterns of the monohydrate-containing 24-h films after the conversion heat treatment. The monohydrate phase observed in the 24-h films in Figure 1 has completely disappeared, giving rise to intense peaks associated with the perovskite phase. The samples were completely converted back to the perovskite structure regardless of the degradation level, showing no traces of the monohydrate phase. Figure 3 also shows that the monohydrate phase disappeared by forming more perovskite, since no PbI_2 was detected. This should be expected since the conversion heat treatment parameters (100 °C for 10 s) were chosen so as to remove water from the monohydrate without inducing any PbI_2 formation via thermal degradation.

To confirm the complete removal of water in the treated perovskite 24-h films, FTIR analyses were carried out on the sample deposited at 100 °C and annealed for 30 s, before and after the heat treatment. The results are shown in Figure 4. The spectrum of the untreated 24-h film shows peaks (indicated by arrows) that are associated with O-H bonds³¹. The presence of these peaks suggests that water is bonded to the perovskite structure, confirming the presence of the monohydrate phase. The O-H peaks are absent in the spectrum of the heat-treated 24-h film, which exhibits, instead, the peaks associated with the perovskite structure, as shown in Table 2^{37,38}. It is important to emphasize that reversible degradation changes both the structure and the color of the film. When fully degraded into monohydrated perovskite, the films are transparent, but they are converted back to the typical dark color of the perovskite after the heat treatment.

To verify whether the perovskite 24-h films would reversibly degrade when exposed to humidity for long times,

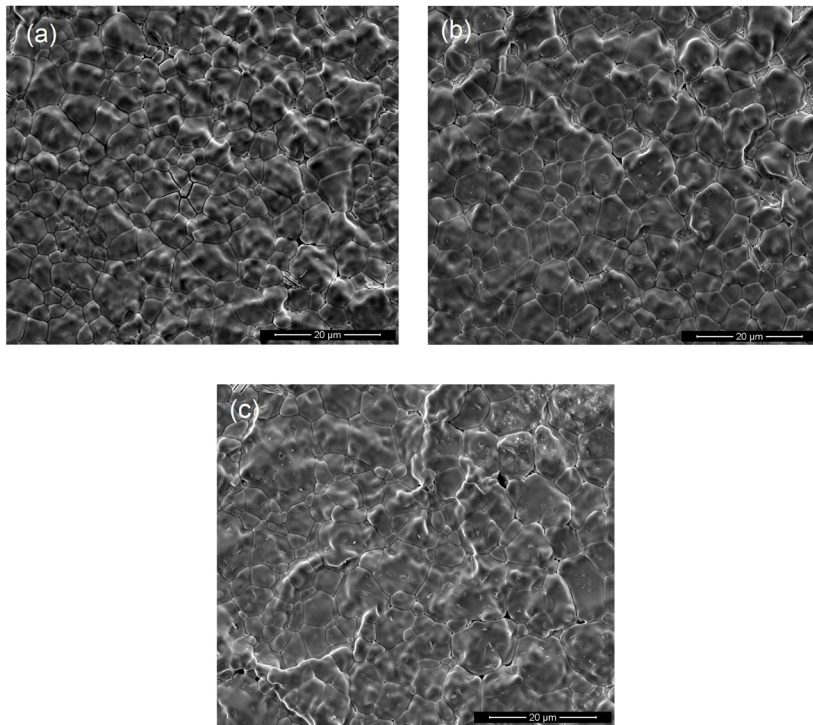


Figure 2. SEM images of the perovskite 24-h films fabricated via spray deposition at 120 °C and annealed for: a) 10 s; b) 20 s; c) 30 s.

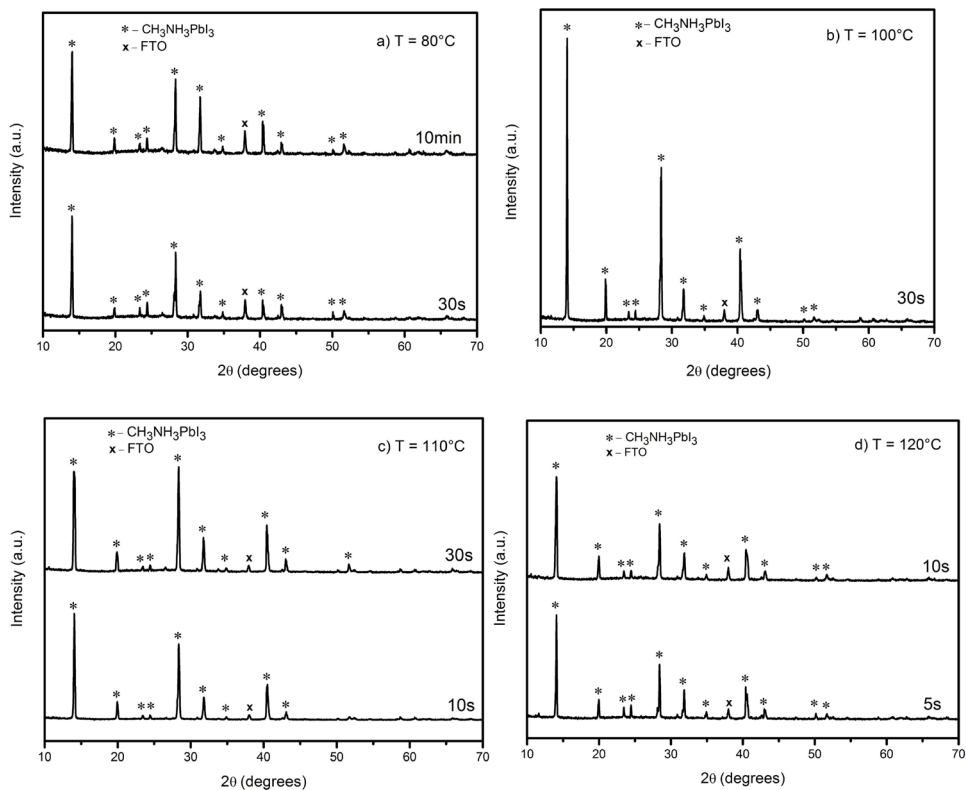


Figure 3. XRD patterns of the treated perovskite 24-h films fabricated via spray deposition at different temperatures and annealing times: a) 80 °C; b) 100 °C; c) 110 °C; d) 120 °C.

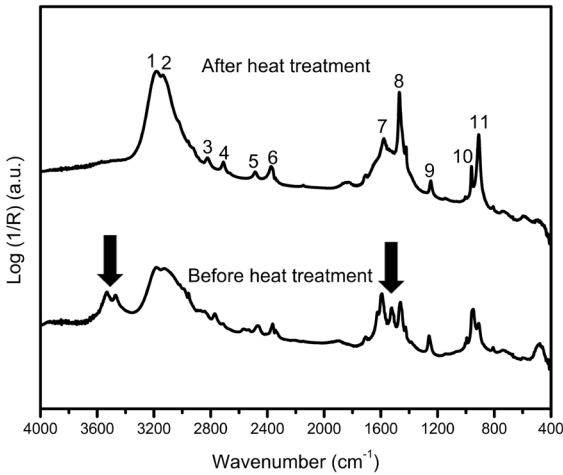


Figure 4. FTIR spectra of the perovskite 24-h films fabricated via spray deposition at 100 °C and annealed for 30 s before and after heat treatment.

Table 2. FTIR peak assignments of the $\text{CH}_3\text{NH}_3\text{PbI}_3$ perovskite thin films.

Peak	Wavenumber (cm ⁻¹)	Vibrational modes
1	3183	asym. NH_3^+ stretch
2	3138	sym. NH_3^+ stretch
3	2823	antisym. NH_3^+ deformation + rock
4	2711	sym. NH_3^+ deformation + rock
5	2485	2 x rock
6	2374	C-N stretch + CH_3 antisym. deformation
7	1578	asym. NH_3^+ bend
8	1469	sym. NH_3^+ bend
9	1248	CH_3 - NH_3^+ rock
10	959	C-N stretch
11	909	CH_3 - NH_3^+ rock

all films were kept under ambient conditions for 50 days. Figure 5 depicts the XRD results of the 50-day films in the range of 10° to 15° (range of interest for identification of the monohydrate phase). The monohydrate phase was present in all films except those deposited at 110 °C for 1 min and 120 °C for 30 s. The diffractograms reveal a similar trend to the one observed in Figure 1, that is, samples deposited at higher temperatures and annealed for longer times (110 °C for 1 min and 120 °C for 30 s) show no sign of reversible degradation. Interestingly, these samples were the ones that underwent partial irreversible degradation via precipitation of a small amount of PbI_2 during deposition, confirming that the presence of PbI_2 affords protection against reversible degradation. However, some PbI_2 content is also found in the films that had not undergone partial irreversible degradation during the deposition process, e.g. the films deposited at 80 °C, suggesting that irreversible degradation took place in the 50-day films due to the prolonged exposure to moisture.

Figure 5 also shows that some of the 50-day films that had not exhibited the monohydrate phase (for example, the 24-h films at 100 °C for 1 min, 100 °C for 3 min, and 120 °C for 20 s in Figure 1) now show traces of reversible degradation. Additionally, no dihydrate phase was found in these samples, suggesting that it is not thermodynamically stable under high humidity³⁶ or that it formed, but disappeared over the 50-day period.

The XRD results of the monohydrate-containing 50-day films submitted to the conversion heat treatment are shown in Figure 6. The monohydrate phase disappeared and all samples were converted back to perovskite. Unlike the 24-h films, the 50-day films contained a significant amount of PbI_2 that remained after the heat treatment. Therefore, the statement that the heat treatment removes the monohydrate phase without inducing PbI_2 via thermal degradation is not so straightforward in these samples. However, it is unlikely that a 100 °C heat treatment carried out for 10 s led to formation of PbI_2 , since at this temperature thermal degradation would only have been triggered after 3 min, as indicated in Figure 1.

SEM images in Figure 7 show the surface morphology of some of the treated 50-day films. Different microstructures are observed in these converted samples and this result may give some insight into the degradation mechanism. Figure 7a shows the morphology of the sample deposited at 120 °C and annealed for 5 s (the one that, before heat treatment, was fully degraded into the monohydrate phase, as confirmed by the diffractograms shown in Figures 1 and 5). The surface is composed of highly oriented grains, a typical morphology that was found in untreated films, indicating that even after reversing back to perovskite, the morphology remained unchanged. The non-reversibility of the microstructure may limit the perovskite properties and needs to be further investigated. Figure 7b shows the morphology of a treated 50 day-film (deposited at 120 °C, annealed for 20 s), the one that before heat treatment was composed by three phases, namely perovskite, monohydrated perovskite, and PbI_2 . All morphologies can be seen in this image: i) irreversible PbI_2 , due to the 50-day exposure to ambient conditions; ii) monohydrated perovskite, with highly oriented grains, typical of reversible degradation; iii) perovskite with no sign of degradation. Every morphology was confirmed by a SEM analysis performed in single phase samples. Therefore, although Figure 6d confirms the conversion of the monohydrate phase back to perovskite, the morphology remained unchanged after heat treatment. On the other hand, the microstructure of the sample deposited at 120 °C and annealed for 30 s (the one where, before heat treatment, no monohydrate phase was detected by XRD), is formed by equiaxed grains, with PbI_2 precipitates inside the grain (Figure 7c). Figure 7d shows another area of the same sample where one can see the typical morphology of monohydrated perovskite. Since the monohydrate phase was not detected in the XRD diffractograms of this sample, it is possible that it has been formed initially, but subsequent growth has been prevented by the presence of PbI_2 . Therefore, it can be argued that a thin layer of PbI_2 is effective to prevent reversible degradation.

Figure 8 shows a summary of the extra phases (PbI_2 and/or monohydrate) found in all perovskite films after the

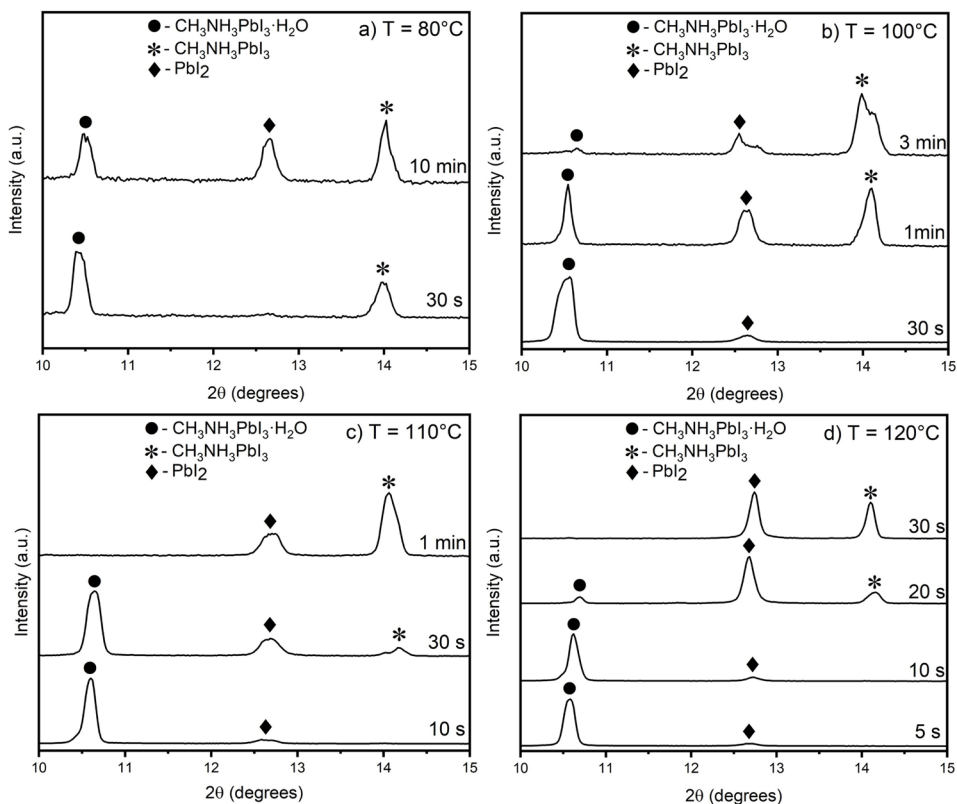


Figure 5. XRD patterns of the perovskite 50-day films fabricated via spray deposition at different temperatures and annealing times: a) 80 °C; b) 100 °C; c) 110 °C; d) 120 °C.

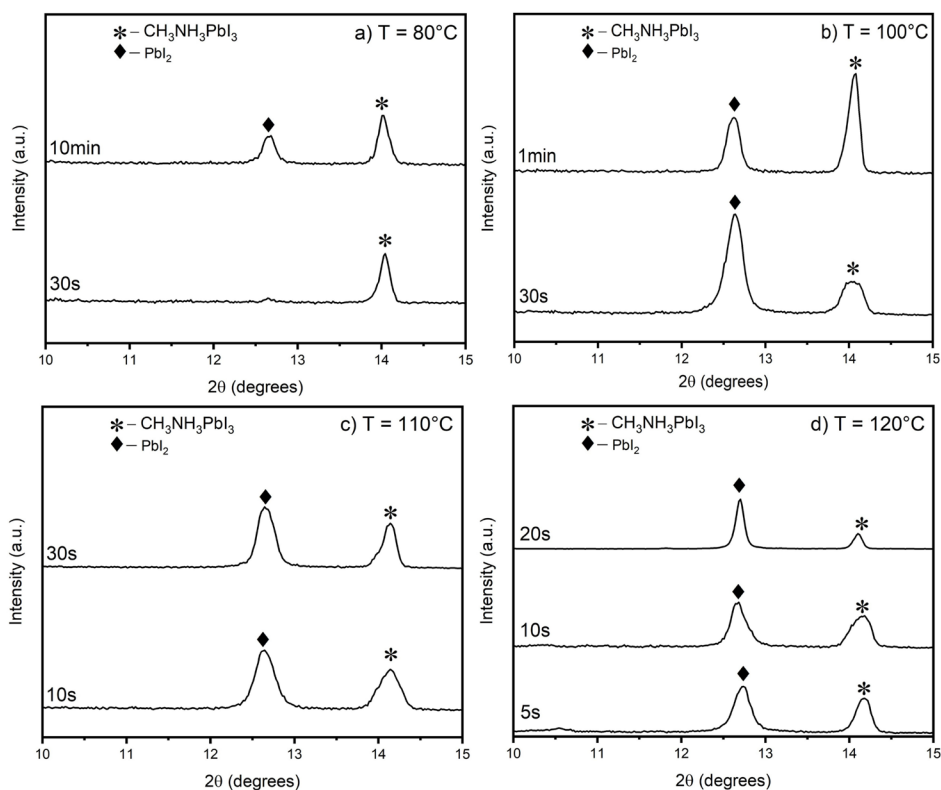


Figure 6. XRD patterns of the treated perovskite 50-day films fabricated via spray deposition at different temperatures and annealing times: a) 80 °C; b) 100 °C; c) 110 °C; d) 120 °C.

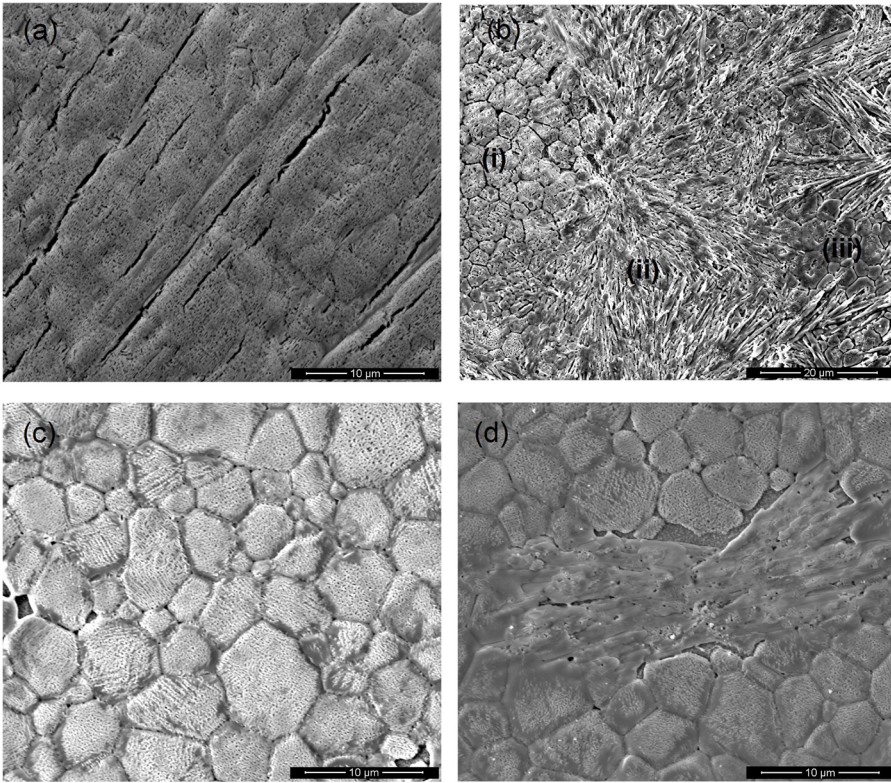


Figure 7. SEM images of the treated perovskite 50-day films fabricated via spray deposition at 120 °C and annealed for: a) 5 s; b) 20 s, showing irreversible PbI_2 (i), reversible monohydrate (ii), and perovskite (iii); c) 30s; d) 30 s, different area.

Before heat treatment							
80 °C		100 °C		110 °C		120 °C	
24 h	50 d	24 h	50 d	24 h	50 d	24 h	50 d
30 s		30 s		10 s		5 s	
mono	mono	mono	mono PbI_2	mono	mono PbI_2	mono	mono PbI_2
10 min		1 min		30 s		10 s	
mono	mono PbI_2	—	mono PbI_2	mono	mono PbI_2	mono	mono PbI_2
30 s		3 min		1 min		20 s	
—	—	PbI_2	mono PbI_2	PbI_2	PbI_2	—	mono PbI_2
30 s		30 s		30 s		30 s	
PbI_2	PbI_2	PbI_2	PbI_2	PbI_2	PbI_2	PbI_2	PbI_2
After heat treatment							
80 °C		100 °C		110 °C		120 °C	
24 h	50 d	24 h	50 d	24 h	50 d	24 h	50 d
30 s		30 s		10 s		5 s	
—	—	—	PbI_2	—	PbI_2	—	PbI_2
10 min		1 min		30 s		10 s	
—	PbI_2	x	PbI_2	—	PbI_2	—	PbI_2
30 s		3 min		1 min		20 s	
—	—	x	PbI_2	x	x	x	PbI_2
30 s		30 s		30 s		30 s	
x	x	x	x	x	x	x	x

Figure 8. Evolution of extra phases in perovskite films after exposure to high humidity for 24 h and 50 days, before and after the conversion heat treatment: monohydrate (mono); PbI_2 ; no extra phases (—); no treatment (x).

degradation procedures (24 h and 50 days), before and after the conversion heat treatment. It is evident that the films deposited at higher temperatures and annealed for longer times (e.g., 100 °C for 3 min, 110 °C for 1 min and 120 °C for 30 s) contained the PbI_2 phase and did not degrade to monohydrated perovskite over the first 24 h. Even after 50 days, these films were still free of the monohydrate phase except for the 100 °C/3min film, that showed traces of this hydrate (Figure 5) - confirming that a small amount of PbI_2 prevented or retarded the formation of the monohydrate phase. In addition, it can be seen that the treatment was efficient for removing the monohydrate phase in all films.

We consider that the films deposited at 120 °C and annealed for 30s are the most adequate for solar cell manufacturing, since they contain only a small amount of PbI_2 (and therefore do not undergo reversible degradation) while exhibiting high coverage and large grains³³. The small amount of PbI_2 that is present in these films should not impair the cell efficiency. In fact, the literature has shown that cells with residual PbI_2 in the perovskite layer may yield a better performance³⁹.

4. Conclusions

Perovskite films were fabricated by the spray deposition method using different deposition temperatures and annealing times. Due to the exposure to high humidity, most of perovskite films exhibited the monohydrate phase - typical of reversible degradation - within the first 24 hours, but samples fabricated at the highest temperature for long annealing times exhibited a low level of degradation or no degradation. XRD results suggest that a small amount of PbI_2 formed during deposition gives rise to a protective layer that prevents moisture from interacting with perovskite to form monohydrated perovskite. Additionally, these perovskite films were still free of the monohydrate phase even after 50 days of high humidity exposure. No sign of the dihydrate phase was found in these samples indicating that it was thermodynamically unstable under high humidity or that it was formed, but disappeared over the 50-day period.

5. Acknowledgments

This work was supported by *Conselho Nacional de Desenvolvimento Científico e Tecnológico* (CNPq) and *Fundação de Amparo à Pesquisa do Estado do Rio de Janeiro* (FAPERJ). We thank the *Laboratório Multiusuário de Espectroscopia da Universidade Federal Fluminense* (LAME-UFF) for the diffuse reflectance IR spectra and the *Laboratório Multiusuário de Difração de Raios X da Universidade Federal Fluminense* (LDRX-UFF) for the XRD diffractograms.

6. References

- Green M, Dunlop E, Hohl-Ebinger J, Yoshita M, Kopidakis N, Hao X. Solar cell efficiency tables (version 57). *Prog Photovolt Res Appl*. 2021;29:3-15.
- Xiao J, Shi J, Li D, Meng Q. Perovskite thin-film solar cell: excitation in photovoltaic science. *Sci China Chem*. 2015;58:221-38.
- Stranks SD, Eperon GE, Grancini G, Menelaou C, Alcocer MJP, Leijtens T, et al. Electron-hole diffusion lengths exceeding 1 micrometer in an organometal trihalide perovskite absorber. *Science*. 2013;342:341-4.
- Snaith HJ. Perovskites: the emergence of a new era for low-cost, high-efficiency solar cells. *J Phys Chem Lett*. 2013;4:3623-30.
- Walsh A. Principles of chemical bonding and band gap engineering in hybrid organic-inorganic halide perovskites. *J Phys Chem C*. 2015;119:5755-60.
- Xing G, Mathews N, Sun S, Lim SS, Lam YM, Gratzel M, et al. Long-range balanced electron- and hole-transport lengths in organic-inorganic $\text{CH}_3\text{NH}_3\text{PbI}_3$. *Science*. 2013;342:344-7.
- Ono LK, Leyden MR, Wang S, Qi Y. Organometal halide perovskite thin films and solar cells by vapor deposition. *J Mater Chem A Mater Energy Sustain*. 2016;4:6693-713.
- Fan P, Gu D, Liang G, Luo J, Chen J, Zheng Z, et al. High-performance perovskite $\text{CH}_3\text{NH}_3\text{PbI}_3$ thin films for solar cells prepared by single-source physical vapour deposition. *Sci Rep*. 2016;6:29910.
- Wang Q, Shao Y, Dong Q, Xiao Z, Yuan Y, Huang J. Large fill-factor bilayer iodine perovskite solar cells fabricated by a low-temperature solution-process. *Energy Environ Sci*. 2014;7:2359-65.
- Ramesh M, Boopathi KM, Huang T, Huang Y, Tsao C, Chu C. Using an airbrush pen for layer-by-layer growth of continuous perovskite thin films for hybrid solar cells. *ACS Appl Mater Interfaces*. 2015;7:2359-66.
- Bishop JE, Mohamad DK, Wong-Stringer M, Smith A, Lidzey DG. Spray-cast multilayer perovskite solar cells with an active-area of 1.5 cm². *Sci Rep*. 2017;7:7962.
- Im J, Kim H, Park N. Morphology-photovoltaic property correlation in perovskite solar cells: one-step versus two-step deposition of $\text{CH}_3\text{NH}_3\text{PbI}_3$. *APL Mater*. 2014;2:081510.
- Jeon NJ, Noh JH, Kim YC, Yang WS, Ryu S, Seok SI. Solvent engineering for high-performance inorganic-organic hybrid perovskite solar cells. *Nat Mater*. 2014;13:897-903.
- Xiao M, Huang F, Huang W, Dkhissi Y, Zhu Y, Etheridge J, et al. A fast deposition-crystallization procedure for highly efficient lead iodide perovskite thin-film solar cells. *Angew Chem Int Ed*. 2014;53:9898-903.
- Liang Z, Zhang S, Xu X, Wang N, Wang J, Wang X, et al. A large grain size perovskite thin film with a dense structure for planar heterojunction solar cells via spray deposition under ambient conditions. *RSC Advances*. 2015;5:60562-9.
- Barrows AT, Pearson AJ, Kwak CK, Dunbar ADF, Buckley AR, Lidzey DG. Efficient planar heterojunction mixed-halide perovskite solar cells deposited via spray-deposition. *Energy Environ Sci*. 2014;7:2944-50.
- Bi Z, Liang Z, Xu X, Chai Z, Jin H, Xu D, et al. Fast preparation of uniform large grain size perovskite thin film in air condition via spray deposition method for high efficient planar solar cells. *Sol Energy Mater Sol Cells*. 2017;162:13-20.
- Mohamad DK, Griffin J, Bracher C, Barrows AT, Lidzey DG. Spray-cast multilayer organometal perovskite solar cells fabricated in air. *Adv Energy Mater*. 2016;6:1600994.
- Giroto C, Moia D, Rand B, Heremans P. High-performance organic solar cells with spray-coated hole-transport and active layers. *Adv Funct Mater*. 2010;21:64-72.
- Eslamian M. Spray-on thin film PV solar cells: advances, potentials and challenges. *Coatings*. 2014;4:60-84.
- Bryant D, Aristidou N, Pont S, Sanchez-Molina I, Chotchunangatchaval T, Wheeler S, et al. Light and oxygen induced degradation limits the operational stability of methylammonium lead triiodide perovskite solar cells. *Energy Environ Sci*. 2016;9:1655-60.
- Lee S, Kim S, Bae S, Cho K, Chung T, Mundt LE, et al. UV degradation and recovery of perovskite solar cells. *Sci Rep*. 2016;6:38150.

23. Niu G, Guo X, Wang L. Review of recent progress in chemical stability of perovskite solar cells. *J Mater Chem A Mater Energy Sustain*. 2015;3:8970-80.
24. Matteucci F, Cinà L, Lamanna E, Cacovich S, Divitini G, Midgley PA, et al. Encapsulation for long-term stability enhancement of perovskite solar cells. *Nano Energy*. 2016;30:162-72.
25. Guarnera S, Abate A, Zhang W, Foster JM, Richardson G, Petrozza A, et al. Improving the long-term stability of perovskite solar cells with a porous Al₂O₃ buffer layer. *J Phys Chem Lett*. 2015;6:432-7.
26. Bai S, Da P, Li C, Wang Z, Yuan Z, Fu F, et al. Planar perovskite solar cells with long-term stability using ionic liquid additives. *Nature*. 2019;571:245-50.
27. Leguy AMA, Hu Y, Campoy-Quiles M, Alonso MI, Weber OJ, Azarhoosh P, et al. Reversible hydration of CH₃NH₃PbI₃ thin films, single crystals, and solar cells. *Chem Mater*. 2015;27:3397-407.
28. Yang J, Siempelkamp BD, Liu D, Kelly TL. Investigation of CH₃NH₃PbI₃ degradation rates and mechanisms in controlled humidity environments using in situ techniques. *ACS Nano*. 2015;9(2):1955-63.
29. Wang Q, Chen B, Liu Y, Deng Y, Bai Y, Dong Q, et al. Scaling behavior of moisture-induced grain degradation in polycrystalline hybrid perovskite thin films. *Energy Environ Sci*. 2017;10:516-22.
30. Christians JA, Miranda Herrera PA, Kamat PV. Transformation of the excited state and photovoltaic efficiency of CH₃NH₃PbI₃ perovskite upon controlled exposure to humidified air. *J Am Chem Soc*. 2015;137:1530-8.
31. Halder A, Choudhury D, Ghosh S, Subbiah AS, Sarkar SK. Exploring thermochromic behavior of hydrated hybrid perovskites in solar cells. *J Phys Chem Lett*. 2015;6:3180-4.
32. Shahbazi M, Wang H. Progress in research on the stability of organometal perovskite solar cells. *Sol Energy*. 2016;123:74-87.
33. Bartholazzi G, Pereira RP, Lima AM, Pinheiro WA, Cruz LR. Influence of substrate temperature on the chemical, microstructural and optical properties of spray deposited CH₃NH₃PbI₃ perovskite thin films. *J Mater Res Technol* 2020;9:3411-7.
34. Oku T. Crystal structures of perovskite halide compounds used for solar cells. *J Adv Mater Sci*. 2020;59:264-305.
35. Shkir M, Abbas H, Siddhartha, Khan ZR. Effect of thickness on the structural, optical and electrical properties of thermally evaporated PbI₂ thin films. *J Phys Chem Solids*. 2012;73:1309-13.
36. Petrus ML, Hu Y, Moia D, Calado P, Leguy AMA, Barnes PRF, et al. The influence of water vapor on the stability and processing of hybrid perovskite solar cells made from non-stoichiometric precursor mixtures. *ChemSusChem*. 2016;9:2699-707.
37. Glaser T, Müller C, Sendner M, Krekeler C, Semonin OE, Hull TD, et al. Infrared spectroscopic study of vibrational modes in methylammonium lead halide perovskites. *J Phys Chem Lett*. 2015;6:2913-8.
38. Oxtou IA, Knop O, Duncan JI. The infrared spectrum and force field of the methyl-ammonium ion in (CH₃NH₃)₂PtCl₆. *J Mol Struct*. 1977;38:25-32.
39. Shi B, Yao X, Hou F, Guo S, Li Y, Wei C, et al. Unraveling the passivation process of PbI₂ to enhance the efficiency of planar perovskite solar cells. *J Phys Chem C*. 2018;122:21269-76.